Wrist-to-Wrist Bioimpedance Can Reliably Detect Discrete Self-Touch

Forte, Maria Paola; Vardar, Yasemin; Javot, Bernard; Kuchenbecker, Katherine J.

DOI
10.1109/TIM.2025.3544385

Publication date
2025

Document Version
Final published version

Published in
IEEE Transactions on Instrumentation and Measurement

Citation (APA)
Forte, M. P., Vardar, Y., Javot, B., & Kuchenbecker, K. J. (2025). Wrist-to-Wrist Bioimpedance Can Reliably Detect Discrete Self-Touch. *IEEE Transactions on Instrumentation and Measurement*, *74*, Article 4006511. https://doi.org/10.1109/TIM.2025.3544385

Wrist-to-Wrist Bioimpedance Can Reliably Detect Discrete Self-Touch

Maria-Paola Forte, *Graduate Student Member, IEEE*, Yasemin Vardar, *Member, IEEE*, Bernard Javot, *Member, IEEE*, and Katherine J. Kuchenbecker, *Fellow, IEEE*

***Abstract*— Self-touch is crucial in human communication, psychology, and disease transmission, yet existing methods for detecting self-touch are often invasive or limited in scope. This study systematically investigates the feasibility of using noninvasive electrical bioimpedance for detecting discrete self-touch poses across individuals. While previous research has focused on classifying defined self-touch poses, our work explores how various poses cause bioimpedance changes, providing insights into the underlying physiological mechanisms. We thus created a dataset of 27 genuine self-touch poses, including skin-to-skin contact between the hands and face and skin-to-clothing contact between the hands and chest, alongside six adversarial mid-air gestures. We then measured the wrist-to-wrist bioimpedance of 30 adults (15 females and 15 males) across these poses, with each measurement preceded by a no-touch pose serving as a baseline. Statistical analysis of the measurements showed that skin-to-skin contacts cause significant changes in bioimpedance magnitude between 237.8 kHz and 4.1 MHz, while adversarial gestures do not; skin-to-clothing contacts cause less-significant changes due to the influence and variability of the clothing material. Furthermore, our analysis highlights the sensitivity of bioimpedance to the body parts involved, skin contact area, and individual's characteristics. Our contributions are twofold: 1) we demonstrate that bioimpedance offers a practical, noninvasive solution for detecting self-touch poses involving skin-to-skin contact, and 2) researchers can leverage insights from our study to determine whether a pose can be detected without extensive testing.**

***Index Terms*— Contact detection, electrical bioimpedance spectroscopy (EBIS), human bioimpedance, human–computer interaction, self-touch poses.**

I. Introduction

SELF-TOUCH occurs when an individual uses their hand(s) to make physical contact with another body part, either directly on their skin or through clothing. These actions are often performed with little or no awareness [1], especially when self-touch is the manifestation of a psychological state, such as stress or task concentration [2]. Facial self-touch is a particularly prevalent human behavior, with individuals unconsciously touching their face approximately 50 times per hour [3], usually with their nondominant hand [4]. Self-touch also serves communicative purposes, such as partially covering the eyes to express dismay or covering both ears to indicate noise sensitivity, especially in individuals with autism [5]. In addition, self-touch is integral to sign languages, where many signs involve contact between the left and right hands or between one or both hands and the signer's face or chest [6].

While the human sense of touch can reliably detect the occurrence of a self-touch event, the body parts involved, and the surface area of the skin contact, replicating this level of reconstruction remains challenging for sensing devices. Nonetheless, being able to reconstruct self-touch with sensors could positively impact several fields. For example, it could provide insights into human psychological states and behavior [2], monitor hygiene and virus transmission [7], and enrich wearable or on-skin interfaces [8].

Self-touch can be detected by measuring the user's brain activity with functional magnetic resonance imaging (fMRI) [9]. This method allows scientists to investigate the brain activity related to self-touch but is unsuitable for other applications because of the size, cost, and complexity of fMRI machines. Alternatively, self-touch can be sensed using electronic skin (e-skin) technologies, which can detect the exact location and force of touch. However, e-skin must cover large areas of the body with the sensing device, reducing comfort and practicality for long-term use [10].

Without direct instrumentation, self-touch can be estimated by having a human observer manually annotate each individual event [7], which is time-consuming, error-prone, expensive, and difficult to scale. Vision-based methodologies, in which the hand pose and self-contacts are reconstructed from RGB or RGB-D videos [11], [12], [13], [14], [15], face challenges when distinguishing contact from close proximity, especially from arbitrary viewing angles. In addition, continuous video capture in good lighting conditions is not realistic for everyday situations.

Many of the limitations identified for observer-based and vision-based approaches can be overcome by using small wearable sensors that detect the user's wrist accelerations [1], muscular activation [1], ultrasound propagation [8], [16], conductivity [17], electrical bioimpedance [18], or hand proximity [19]. Among these modalities, we chose to investigate bioimpedance using electrical bioimpedance spectroscopy (EBIS). Bioimpedance sensing has been widely used to assess

Received 29 July 2024; revised 15 October 2024; accepted 9 November 2024. Date of publication 21 February 2025; date of current version 8 April 2025. This work was supported by the Max Planck Society. The Associate Editor coordinating the review process was Dr. Yandan Jiang. *(Corresponding author: Maria-Paola Forte.)*

Maria-Paola Forte, Bernard Javot, and Katherine J. Kuchenbecker are with the Haptic Intelligence Department, Max Planck Institute for Intelligent Systems, 70569 Stuttgart, Germany (e-mail: forte@is.mpg.de; javot@is.mpg.de; kjk@is.mpg.de).

Yasemin Vardar is with the Department of Cognitive Robotics, Delft University of Technology, 2628 CD Delft, The Netherlands (e-mail: Y.Vardar@tudelft.nl).

Digital Object Identifier 10.1109/TIM.2025.3544385

body composition [20] and more recently as a noninvasive approach for several medical applications, such as pulmonary nodule identification [21], edema supervision for heart failure [22], health assessment of cerebral blood flow [23], blood pressure monitoring [24], and insulin measurement [25]. Beneficially, a bioimpedance-based system: 1) does not encumber the user's hands or face, 2) has the potential to quickly detect very small changes in the contact [26], and 3) could be embedded in a wearable device. So far, previous work has largely focused on developing algorithms for detecting contact at specific body locations and classifying defined gestures. Furthermore, key factors such as sex, ethnicity, and body mass index (BMI), which significantly affect bioimpedance [27], [28], have not been explicitly considered.

To address this gap and enable scalable self-touch detection, our research focuses on a fundamental question: Which *types of* discrete self-touch poses, *if any*, can bioimpedance-based systems reliably detect across diverse individuals? To answer this question, we created a dataset consisting of 27 genuine self-touch poses and six adversarial mid-air gestures collected from 30 participants. We then measured the participants' bioimpedance across a wide range of frequencies by connecting two conductive wristbands to an impedance analyzer, replicating the setup used by Touché [18] to classify five poses. We finally conducted a detailed analysis of how the 33 poses of our dataset affect bioimpedance compared to the individual's baseline. This makes our study the first to systematically link self-touch poses to changes in bioimpedance. We also examined the sensitivity of bioimpedance changes to factors such as the body parts involved, the surface area of skin contact, individual characteristics, and external conditions.

Our results show that bioimpedance-based sensing systems hold great promise for reliably detecting skin-to-skin self-touch poses. We identified the specific range of bioimpedance frequencies that are most informative for detecting genuine self-touch only, showing that just the magnitude of bioimpedance at high frequencies needs to be observed to accurately infer these events. Furthermore, we found that bioimpedance changes are strongly influenced by key properties of the contact, such as the body parts involved and the skin contact area. These insights lay the foundation for developing more effective and scalable touch-detection systems that use bioimpedance as the sensing modality, helping researchers determine whether a pose can be detected with bioimpedance without extensive additional testing.

II. Sensing Principle: Bioimpedance

The chosen sensing principle leverages the electrical conductivity of the human body to detect a self-touch pose. In general, the impedance (Z) between two points shows how strongly the intervening circuit opposes the flow of an alternating current ($Z = V/I$). Impedance is a complex number that combines resistance (R, real part) and reactance (X, imaginary part). It thus consists of two frequency-dependent components: magnitude ($|Z| = (R^2 + X^2)^{1/2}$) and phase angle ($\angle Z = \tan^{-1}(X/R)$) [29].

Bioimpedance, in turn, is the impedance of a biological medium. Here, the resistance is caused by the total body water, which is moderately conductive, and the reactance is caused mainly by the organism's cell membranes, which act like capacitors [30].

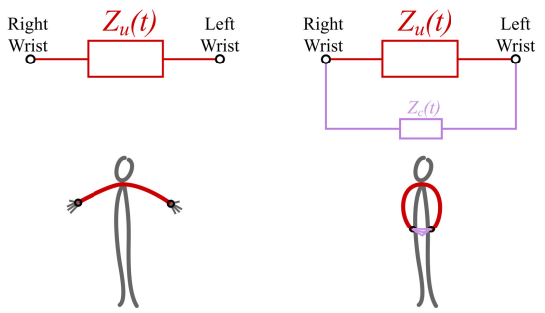

Fig. 1. Bioimpedance of the user's body can be measured from wrist to wrist (Z_u). Forming a new electrical pathway between the wrists, such as when the hands contact each other, can be modeled by an additional bioimpedance component in parallel with the original one (Z_c), as shown on the right. We define both impedance values as functions of time ($Z(t)$) because the bioimpedance of a person changes continuously.

The bioimpedance measured between two anatomical locations (such as the wrists) varies significantly between people because it depends on the shape and composition of their bodies [31]. It even varies within one person because of, for example, changes in skin temperature, core temperature, body position, muscle contraction, exercise, hydration, and fasting state [32], [33], [34], [35], [36]. Importantly for self-touch, bringing two distinct body parts into contact creates a new pathway through which current can flow in parallel with the default pathway through the body, as shown at right in Fig. 1. This new pathway leads to a decrease in the total bioimpedance following the formula:

$$Z_{\text{total}} = \left(\frac{1}{Z_u} + \frac{1}{Z_c}\right)^{-1} \tag{1}$$

where Z_u is the bioimpedance of the upper body measured between the wrists, and Z_c is the bioimpedance of the path formed by the new contact.

III. Materials and Methods

We conducted an exploratory study to understand how self-touch affects the electrical bioimpedance measured between the left and right wrists in different individuals.

A. Experimental Setup

Two conductive wristbands and a high-quality impedance analyzer (MFIA, Zurich Instruments) were used to precisely measure the participants' bioimpedance, as shown in Fig. 2. Specifically, we used a setup similar to the one employed for conducting segmental bioelectrical impedance analysis (BIA) of the upper body, in which alternating current is transmitted from hand to hand through the chest [37]. Mathews and Jovanov [38] recently also identified this wrist-to-wrist configuration as promising for enabling new wearable bioimpedance applications. As the grounding and source electrodes, we explored wet electrodes as well as more practical dry solutions (with different geometries and materials). Since we found consistent results for both wet and dry electrodes

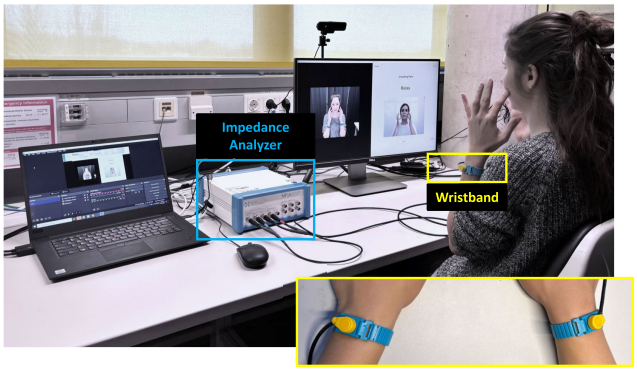

Fig. 2. Experimental setup. The participant wears the wristbands on their left and right wrists. The electrodes in the wristbands are connected to the impedance analyzer through BNC cables. The screen shows the name and a mirrored image of the pose to be mimicked, a message that states whether the participant needs to hold the pose, and their own mirrored video stream captured with an external camera placed above the screen. The laptop computer records the data. The inset shows a top view of both wristbands.

as long as good contact was maintained with the skin, we used commercial anti-static wristbands (ESD Grounding Wrist Strap, 10 mm Stud) with a conductive circumference of 14 cm (when not stretched) to achieve a skin-to-electrode contact area that is both large and stable. The wristbands were connected to the impedance analyzer through shielded cables to reduce noise.

The impedance analyzer was set to operate in four-terminal measurement mode to remove the resistive effect of the wires. We used a parallel resistance and capacitance as the equivalent circuit and a high-accuracy sweep [39]. We used EBIS to measure the wrist-to-wrist impedance of the participant from 100 Hz to 5.1 MHz over 100 logarithmically spaced frequencies. The selected frequency range was chosen to include and extend beyond all frequencies commonly used for BIA. Single-frequency BIA typically measures the phase angle of the bioimpedance at only 50 kHz [20]. Multifrequency BIA, the most widespread and well-known application of EBIS [40], instead sweeps from 5 to 200 kHz because this range has the highest reproducibility, even though day-to-day coefficients of variation increase for frequencies below 50 kHz [20]. Nonetheless, our goal is different from estimating body composition, and we thus measured the bioimpedance across the full range offered by our impedance analyzer.

The experiments were conducted in a temperature-controlled research laboratory. During the experiment, the participant sat in front of a screen displaying a MATLAB graphical user interface (GUI) with a mirrored image of the pose to mimic, their mirrored video stream to check whether they were performing the pose correctly, and a message that told them whether to hold or release the pose. The experimenter used a nearby laptop computer to record the impedance measurements and the participant's screen.

B. Experimental Protocol

We recruited a total of 30 participants, aged 31.2 ± 6.4 years (mean ± standard deviation). Of these, 15 self-reported to be male and 15 to be female, with six participants being left-handed and the remainder right-handed. The participants represented diverse ethnic backgrounds, including Asian, White, and Hispanic, and had a BMI of 22.9 ± 3.0 kg/m^2. None of them had current or past sensory-motor disabilities. Approval of the experimental procedure for this study was granted by the Ethics Council of the Max Planck Society under the Haptic Intelligence Department's framework agreement (protocol number F013C). All participants provided informed consent to participate in the study before data collection. People not employed by our organization were offered a nominal hourly payment.

At the start of the study, the experimenter introduced the 33 poses and the baseline no-touch pose depicted in Fig. 3. As previously stated, self-touch refers to using one's hand(s) to contact another body part, either on the skin or through clothing, with discrete facial self-touches being particularly common. We thus chose 27 poses (rows 1–5) that involve various levels of skin-to-skin contact (rows 1–4) and skin-to-clothing contact (row 5). Finally, we added three variations of two mid-air hand gestures (rows 6–7) that are commonly used in human–computer-interaction applications [41]: pinching the thumb and index fingers together and clenching all of the fingers into a fist. These adversarial gestures can be performed with either one or both hands. Since they involve within-hand skin-to-skin contact, they might be erroneously detected as self-touch poses by bioimpedance-based self-touch systems. The 34th pose is the no-touch pose, which gives us the baseline for the user's wrist-to-wrist bioimpedance (N; row 8). To better understand the underlying physiological mechanisms, we purposefully selected some poses that have electrical topologies similar to one another (e.g., performing the same action with the left or right hand or with a different number of fingers). For conciseness, the actions of touch, pinch, and clench are labeled with lowercase letters (t, p, and c). Capital letters denote the body parts in contact, i.e., left hand, right hand, face, and chest (L, R, F, and C). A numeral at the end of a touch label indicates the number of fingertips in contact (1, 2, 3, 4, or 5). We standardized the fingers used: 1 means only the index finger; 2 means index and middle; 3 means index, middle, and ring; 4 means index, middle, ring, and pinky; and 5 means all five fingers. When there is no number, the entire hand makes contact, including the full fingers and the palm.

After the experimenter's introduction, the participant practiced the poses to ensure comprehension. They then completed a short training to become familiar with the experimental procedure before data collection. The experiment required the participant to complete three measurement cycles; within each cycle, the GUI presented the 33 poses in random order, and each pose was preceded by the no-touch baseline pose. Recording the baseline bioimpedance before each pose, instead of only once within each cycle, is fundamental to our approach, since the user's bioimpedance changes continuously over time due to internal [34] and external factors (such as changes in room humidity, temperature, and wristband position). Each sweep took about 10 s, and the participant held the pose slightly before and after the sweep. After each pair of bioimpedance measurements, i.e., baseline and pose, the participant could take a short break, and they had a longer break between cycles.

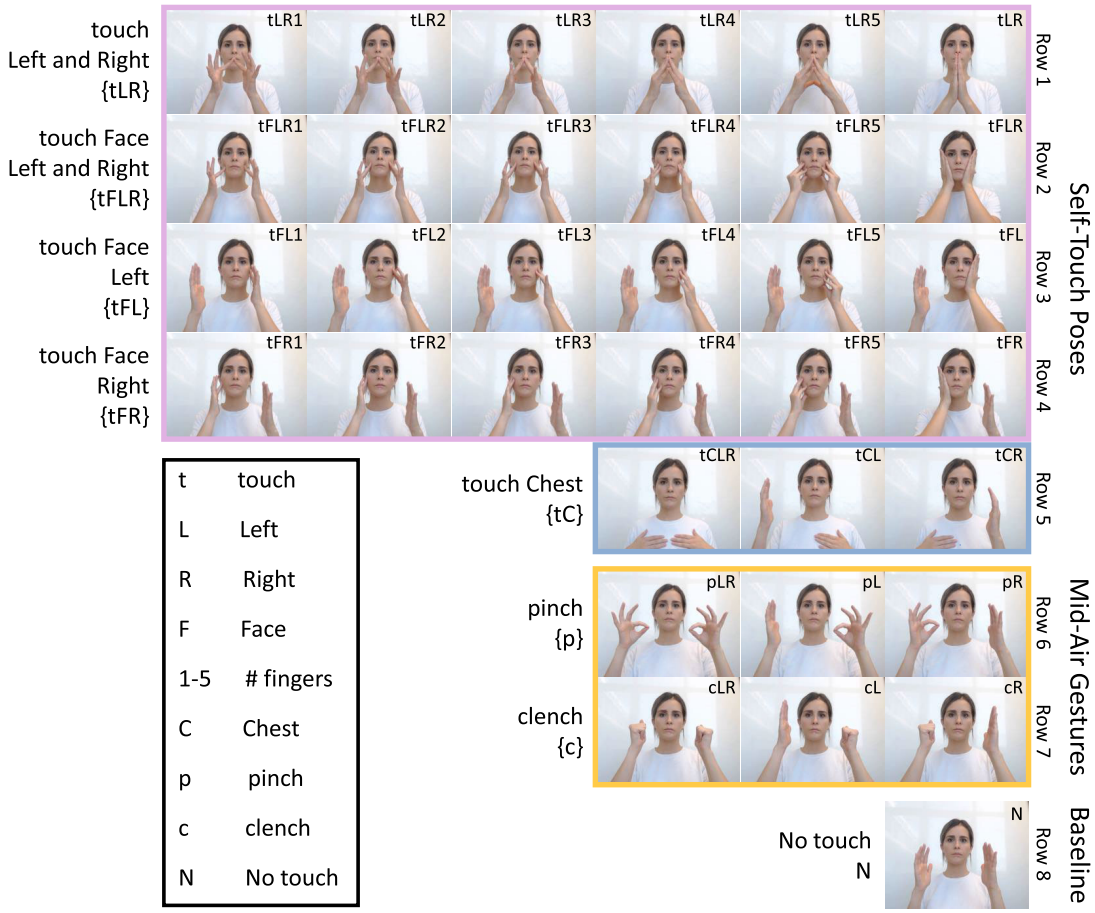

Fig. 3. Poses performed during the experiment. Each row shows a group of related poses, as labeled at the left. The first five rows show self-touch poses; they involve touch interactions between the left and right hands {tLR}, contact with the face by either both hands {tFLR}, the left hand {tFL}, or the right hand {tFR}, and touching the chest with one or both hands {tC}. Skin-to-skin and skin-to-clothing self-touch poses are highlighted in pink and blue, respectively. Rows six and seven show adversarial mid-air gestures: pinching {p} and clenching {c}, performed with either one or both hands. The last row depicts the no-touch condition N.

C. Dataset

The raw dataset includes 1 188 000 data points, which correspond to the magnitude and phase measurements at the 100 frequencies for the 198 trials of each of the 30 participants. In addition, the dataset contains the participants' individual characteristics (i.e., sex, handedness, ethnicity, and BMI), the material of the clothing touched during the chest contacts, and their chosen starting position for the poses (i.e., elbows on the table or in the air). We did not include the age of the participants in the dataset due to its low variability.

The variable indicating the performed pose, i.e., PoseID, has 33 levels (24 skin-to-skin contacts, three skin-to-clothing contacts, and six adversarial mid-air gestures). We refer to all other variables as attributes. Among the attributes, sex, handedness, and starting position have only two levels each. In the case of double ethnicity, we considered the primary one; this choice led to three ethnicity levels: Asian (14 participants), White (14 participants), and Hispanic (two participants). We used the WHO categorization [42] to label the BMI as underweight, normal weight, pre-obesity, and obesity (grouping the three obesity classes together); our participants' BMIs span this full spectrum: one underweight, 21 normal weight, seven pre-obesity, and one obese. Finally, we categorized the clothing materials into three groups. The clothing of six participants did not have any label, so we classified their materials as Unknown. The other two groups were formed based on the clothing conductivity [43]: low-conductivity synthetic polymers, cotton, and linen (24 participants combined) were separated from clothing containing wool (two participants), which is generally more conductive.

After collecting the dataset, we created the new variable ΔBioimpedance that represents the difference between each baseline measurement (the no-touch pose N) and the pose that immediately followed it (i.e., ΔBioimpedance = Baseline − Pose). Over all experimental sessions, ten bioimpedance measurements lacked either the magnitude or the phase at the highest frequency of 5.1 MHz, presumably due to a data-saving error. These ten incomplete data points were thus removed from the dataset, leaving 593 990 magnitude values and 593 990 phase values.

D. Statistical Analysis

We conducted two sets of statistical analyses to understand which types of discrete self-touch poses, if any, bioimpedance-based systems can reliably detect across diverse individuals.

1) Detection of Self-Touch Poses: First, to understand the link between genuine self-touch poses and variations in bioimpedance across individuals, we analyzed the collected

data using the following mixed-effects model:

$$\begin{aligned}\Delta\text{Bioimpedance} \sim\ & -1 + \text{PoseID} + \text{Sex} + \text{Handedness} \\ & + \text{Ethnicity} + \text{BMI} + \text{ClothingMaterial} \\ & + \text{StartPosition} + (1|\text{ParticipantID})\end{aligned}$$

where ΔBioimpedance is the dependent variable, and PoseID is the independent variable. The impact of individual characteristics (i.e., sex, handedness, ethnicity, and BMI) and external factors (i.e., clothing material and starting position) is analyzed by including them as fixed effects. The ID of the participant is modeled as a random effect to account for within-subject variability, as each participant performed the same poses three times. The model was separately fit for the magnitude and the phase using the "lme4" package in R. Concerns about any potential violations of model assumptions should be alleviated by the robustness of mixed-effects models [44]. After confirming the overall significance of each fixed effect with a Type II Wald chi-square test, we performed a false discovery rate post-hoc correction; this particular correction was chosen due to the exploratory nature of this analysis [45].

We deepened our understanding of the influencing factors through a follow-up sensitivity analysis using a leave-one-variable-out approach. In this analysis, we systematically removed one fixed effect at a time, refit the model, and evaluated how the exclusion of each variable impacted the model's performance by examining changes in the conditional and marginal R^2 value, root mean square error (RMSE), Akaike information criterion (AIC), and Bayesian information criterion (BIC).

2) Influence of Body Parts and Skin Contact Area on Skin-to-Skin Bioimpedance Changes: Due to their prevalence and relevance for several application fields, our second analysis focused on the skin-to-skin self-touch poses (rows 1–4 in Fig. 3), aiming to understand how the body parts and skin contact area involved in these contacts influence bioimpedance changes. The 24 poses tested can be divided into either four groups based on the body parts (each group is a row from rows 1–4 in Fig. 3) or six groups based on the contact size (each group is a column from rows 1–4 in Fig. 3). We thus introduced the respective discrete variables TopologyID and ContactAreaID and separately fit the following mixed-effects model to the magnitude and phase of the bioimpedance:

$$\begin{aligned}\Delta\text{Bioimpedance} \sim\ & -1 + \text{TopologyID} * \text{ContactAreaID} \\ & + \text{TopologyID} + \text{ContactAreaID} + \text{Sex} \\ & + \text{Handedness} + \text{Ethnicity} + \text{BMI} \\ & + \text{ClothingMaterial} + \text{StartPosition} \\ & + (1|\text{ParticipantID}).\end{aligned}$$

We then used a Type II Wald chi-square test to check the significance of the interaction effect of TopologyID and ContactAreaID. When the interaction effect was not significant, we analyzed TopologyID and ContactAreaID independently. When significant, we explored the simple effects of each of the two variables at the different levels of the other variable. After confirming the overall significance of each fixed effect with a Type II Wald chi-square test, we corrected the significance using Tukey's HSD for the pairwise comparisons of TopologyID and ContactAreaID and Bonferroni for the attributes.

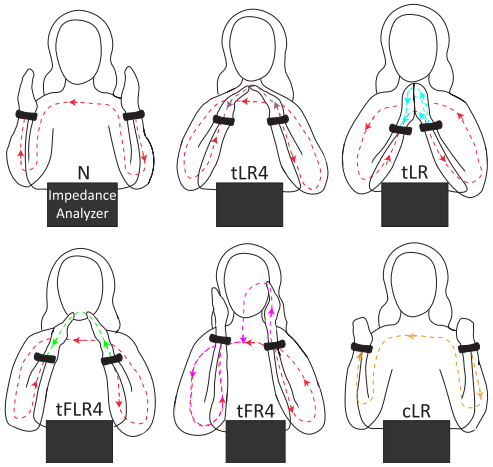

Fig. 4. Mirrored illustrations of current pathways for six sample poses. The red pathway through the user's arms and across their shoulders is always present. Touching the hands together or to the face gives the current a second way to flow from wrist to wrist. Performing a hand gesture like clenching does not alter the circuit topology but might have a somewhat different impedance, shown in yellow.

IV. Results

Fig. 4 shows schematics for the baseline no-touch pose (N) and five other selected poses to illustrate their different conductivity topologies. This set includes four skin-to-skin self-touch poses, i.e., four fingertips of both the left and right hands touching each other (tLR4), the entire hands touching each other (tLR), four fingertips of both the left and right hands touching the face (tFLR4), and four fingertips of only the right hand touching the face (tFR4), as well as one mid-air gesture, i.e., clenching both hands (cLR). For all six of these poses, the three wrist-to-wrist bioimpedance measurements (magnitude and phase across frequencies) from a sample participant are depicted in Fig. 5. The other poses follow similar trends but are omitted for presentation clarity. Both the magnitude and the phase of the measured bioimpedance show systematic differences as a function of frequency. The magnitude decreases with increasing frequency until a change in trend occurs at the highest frequencies, where it rises due to the dominant influence of the parasitic inductance from the cables. In general, it is possible to notice substantial differences between the bioimpedance magnitudes across poses at high frequencies (200 kHz–4.5 MHz, see insets in Fig. 5). The baselines are also relatively stable in this range, hinting that ΔBioimpedance will depend mainly on the pose itself. The bioimpedance phase, instead, seems to differ across poses mainly at the low and middle frequencies, though the baselines also fluctuate greatly in this range.

A. Detection of Self-Touch Poses

Fig. 6 reports the number of fixed effects that caused a significant change in magnitude (see Fig. 6(a)) or phase (see Fig. 6(b)) from the preceding baseline. The PoseID variable is represented by the bars in pink, blue, and yellow (skin-to-skin contacts, skin-to-clothing contacts, and adversarial

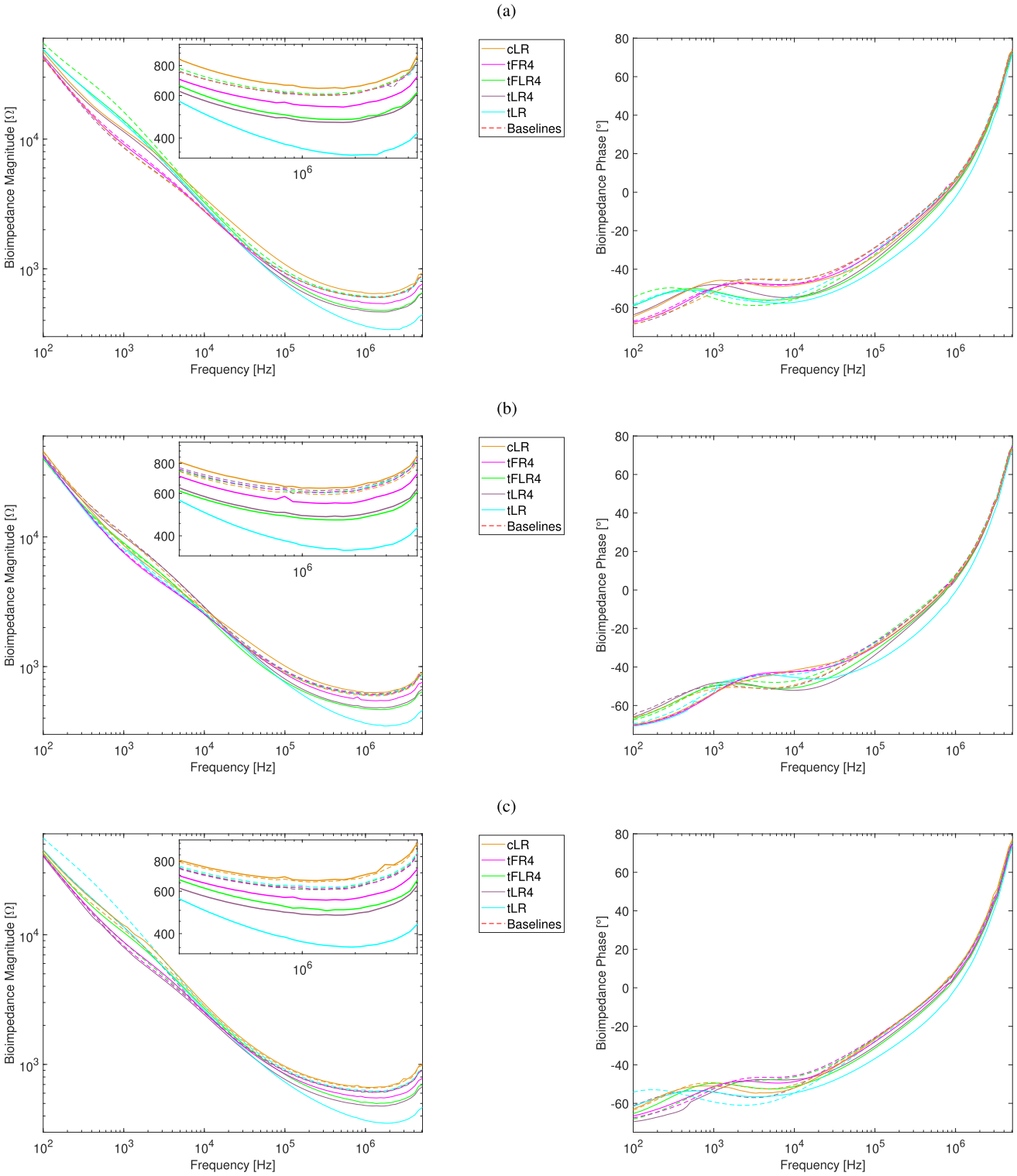

Fig. 5. Wrist-to-wrist bioimpedance of the three cycles of participant 1 for five selected poses (solid lines), i.e., tLR4, tLR, tFLR4, tFR4, cLR, and their respective baselines (dashed lines). The magnitude (left) and phase (right) were measured for (a) Cycle 1, (b) Cycle 2, and (c) Cycle 3 from 100 Hz to 5.1 MHz. The insets in the magnitude plots show the zoomed-in responses from 200 kHz to 4.5 MHz, which are relatively stable across cycles.

mid-air gestures, respectively). The gray bars represent instead the attributes of sex, handedness, ethnicity, BMI, clothing material, and starting position. Lighter color shades indicate significance levels of $p < 0.05$, while darker shades mark $p < 0.001$. We start by analyzing the variable PoseID and then focus on the attributes. This section concludes with the results of the associated sensitivity analysis.

It is important to note that when referring to our results, we use the term "detection" in a statistical sense rather than in the context of machine-learning classification: we refer to significant deviations in bioimpedance from the baseline level.

1) PoseID: As seen in Fig. 6(a), starting at frequency 58 (51.3 kHz), all skin-to-skin poses exhibited a bioimpedance magnitude that significantly differed from the preceding

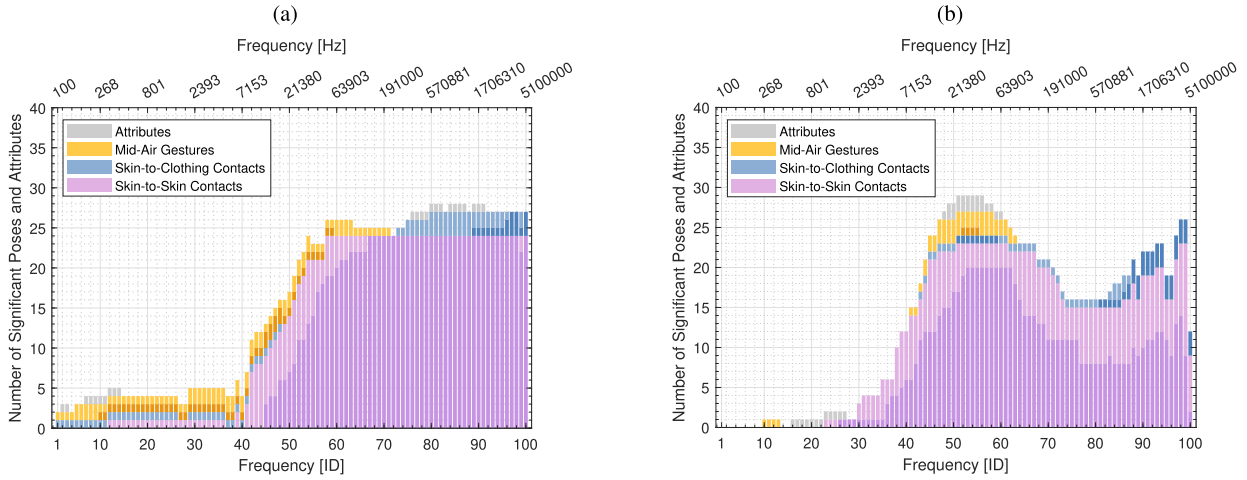

Fig. 6. Stacked bar chart illustrating the number of significant effects on either (a) magnitude or (b) phase of the measured bioimpedance change. Pink refers to the skin-to-skin contacts (maximum 24), blue to the skin-to-clothing contacts (maximum three), and yellow to the mid-air gestures (maximum six). Gray combines all the other fixed effects, i.e., the attributes of sex, handedness, ethnicity, BMI, clothing material, and starting position. The lighter colors show significant differences at $p < 0.05$, and the darker colors mark $p < 0.001$.

baseline ($p < 0.05$). In particular, from approximately 137.5 kHz to 4.1 MHz (from frequency 67 to frequency 98), they were all detected with $p < 0.001$. Starting from frequency 80 (570.9 kHz), all skin-to-clothing contacts also caused significant changes in the bioimpedance ($p < 0.05$), and the significance was $p < 0.001$ at many frequencies for touches performed with two hands (tCLR). When only one hand was used, we observed more detections for the left hand (tCL) than for the right hand (tCR). Among the adversarial mid-air gestures, clenching significantly differed from N ($p < 0.05$) from 100 Hz to 213.1 kHz. Notably, when performed with both hands (cLR) or with the left hand alone (cL), clenching demonstrated substantial significance ($p < 0.001$) across multiple frequencies, with a higher rate of significance observed in the two-hand condition. No pinching pose was detected at any frequency.

In Fig. 6(b), it can be seen that most poses showed a significant deviation in the bioimpedance phase around 50 kHz. In this region, the only skin-to-skin contact that exhibited no significant difference from the baseline was the use of a single fingertip to touch the face (tFR1). All skin-to-clothing poses were detected ($p < 0.001$) starting from 1.4 MHz. Similar to before, among the adversarial mid-air gestures, only a few clench poses were detected (cLR, followed by cR and cL) at low and medium frequencies. Starting from frequency 95 (2.9 MHz), the results became less consistent due to the increased impact of the parasitic inductance on the phase.

2) Attributes: Sex emerged as the only significant attribute ($p < 0.05$) at some low and moderately high frequencies in the magnitude, and had a significant impact ($p < 0.05$) also at low frequencies in the phase. Ethnicity and clothing material significantly affected the bioimpedance phase ($p < 0.05$) in the medium frequencies. Handedness, BMI, and the starting position did not influence the measurements.

3) Sensitivity Analysis: Based on these results, we conducted a sensitivity analysis on only the magnitude and averaged the results within three frequency clusters: low (from 100 Hz to 7.2 kHz), medium (from 8.0 to 213.1 kHz), and high (from 237.8 kHz to 5.1 MHz). Overall, the model with all fixed effects consistently performed best across all metrics, in particular at high frequencies. As expected, PoseID was the most critical predictor; removing it caused dramatic decreases in both conditional and marginal R^2 values (89%–97%) and substantial increases in RMSE, AIC, and BIC. In contrast, removing the other variables led to minor (ethnicity, BMI, and clothing material) or minimal (sex, handedness, and start position) changes in the metrics.

B. Influence of Body Parts and Skin Contact Area on Skin-to-Skin Bioimpedance Changes

We streamline the presentation of our second analysis by reporting results only for $p < 0.05$. We first report the impact of TopologyID and ContactAreaID on the dependent variable ΔBioimpedance and then conclude the section focusing on the attributes (gray bars).

1) TopologyID and ContactAreaID: There was no significant interaction effect between TopologyID and ContactAreaID in the magnitude from frequency 1 (100 Hz) to frequency 51 (23.9 kHz), and in the phase from frequency 1 (100 Hz) until frequency 26 (1.5 kHz), as well as at frequencies 96 (3.3 MHz) and 99 (4.6 MHz).

Fig. 7 shows the results of TopologyID. Until frequency 48 (17.2 kHz), none of the six pairwise comparisons between the four touch topologies ({tFR}, {tFL}, {tFLR}, and {tLR}) showed significant differences in how they changed the bioimpedance magnitude (see Fig. 7(a)). From this frequency to frequency 51 (23.9 kHz), most pairwise comparisons were significant, except for the left- versus right-hand face touch ({tFL} versus {tFR}), which was not significant throughout this range, and between the hands touching directly or through the face ({tFL} versus {tFLR}), which was nonsignificant only at frequency 48. Starting at frequency 52, overall, the pairs comparing the use of one hand with two hands ({tFL} or {tFR} versus {tLR} or {tFLR}) showed significant differences for most frequencies and contact sizes; the less-significant pairwise comparisons were again {tFL} versus {tFR} followed by {tLR} versus {tFLR}. Furthermore, the contact area with

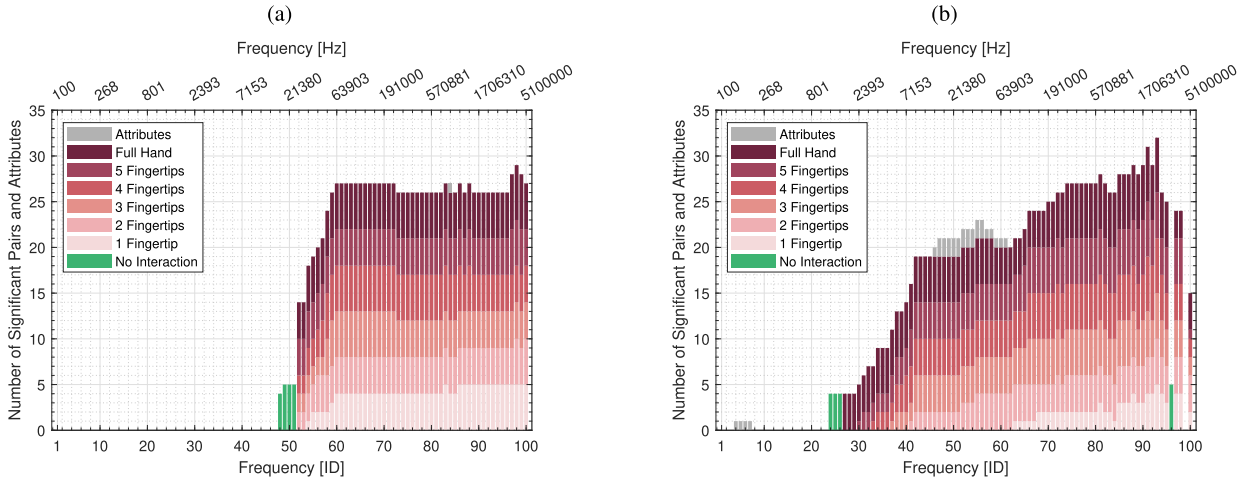

Fig. 7. Stacked bar chart illustrating the number of significant ($p < 0.05$) TopologyID pairwise comparisons and effects for either (a) magnitude or (b) phase of the bioimpedance change (maximum six for each label). The green bars (no interaction) mark the pairwise comparisons that are independent of the ContactAreaID, i.e., when the interaction effect between ContactAreaID and TopologyID is not significant. The other six labels refer to each of the six levels of ContactAreaID, i.e., when the interaction effect between ContactAreaID and TopologyID is significant. Gray combines all the other fixed effects, i.e., the attributes of sex, handedness, ethnicity, BMI, clothing material, and starting position.

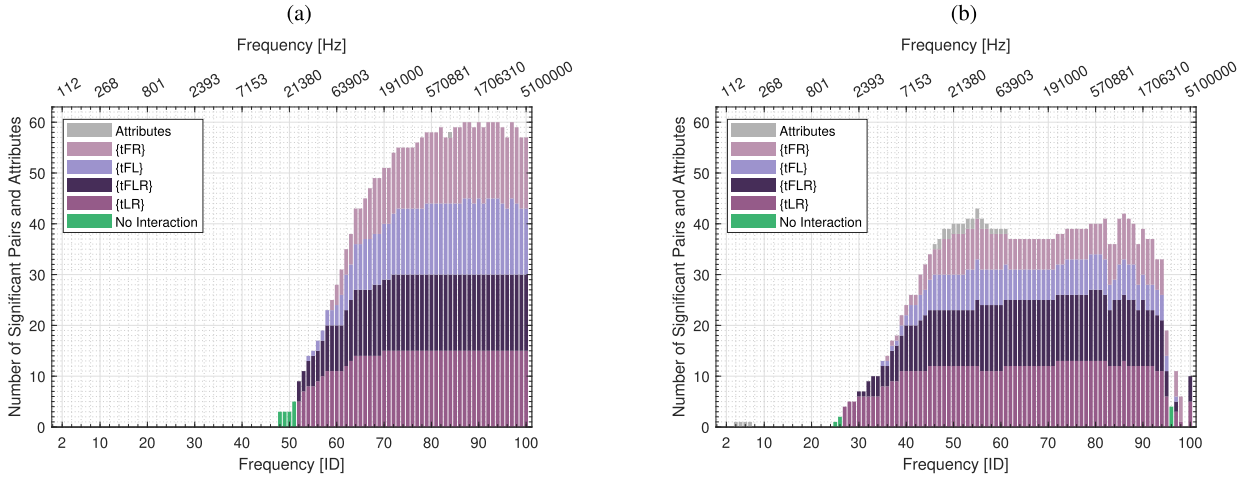

Fig. 8. Stacked bar chart illustrating the number of significant ($p < 0.05$) ContactAreaID pairwise comparisons and effects for either (a) magnitude or (b) phase of the bioimpedance change (maximum 15 for each label). The green bar (no interaction) defines the pairwise comparisons independently of the TopologyID, i.e., when the interaction effect between TopologyID and ContactAreaID is not significant. The other four labels refer to each of the four levels of TopologyID, i.e., when the interaction effect between TopologyID and ContactAreaID is significant. Gray combines all the other fixed effects, i.e., the attributes of sex, handedness, ethnicity, BMI, clothing material, and start position.

the highest number of significant pairwise comparisons was the full hand.

Regarding the phase, as shown in Fig. 7(b), until frequency 24 (1.2 kHz) and at frequency 99 (4.6 MHz), none of the six pairwise comparisons was significant. From frequency 24 (1.2 kHz) to frequency 26 (1.5 kHz), the only nonsignificant comparisons were again {tFL} versus {tFR} and {tLR} versus {tFLR}, with the latter being the only nonsignificant comparison at frequency 96 (3.3 MHz). Starting from frequency 27 (1.7 kHz), overall, the number of significant pairwise comparisons increased proportionally with the frequency and the contact size. At a few high frequencies, all pairwise comparisons were significant when either four or five fingertips were used. With the full hand(s), all comparisons were significant for most of the high frequencies. Starting with frequency 95 (2.9 MHz), the results became less consistent, similar to the behavior witnessed in the first analysis.

Fig. 8 shows the results of ContactAreaID. As the frequency increases, so does the difference in the changes in bioimpedance magnitude between contact sizes. At lower frequencies, only a few pairs with large contact-area differences, e.g., one fingertip versus the full hand, were significantly different. However, at high frequencies all 15 pairwise comparisons were significant when both hands were used, i.e., {tLR} and {tFLR}, and the large majority when only one hand was used, i.e., {tFL} and {tFR}, with some frequencies where all comparisons were significant. The phase followed a similar trend but resulted in fewer significant comparisons, with the number of significant comparisons reducing by about 50% when only one hand was used.

2) Attributes: In the magnitude, only one attribute emerged as significant, and it affected only one frequency: sex at 884.6 kHz. For the phase, the starting position had a significant impact at some very low frequencies, while ethnicity, either

alone or with clothing, had a significant impact at the medium frequencies.

V. Discussion

This study explored the feasibility of using wrist-to-wrist bioimpedance to detect discrete self-touch poses, focusing on both skin-to-skin and skin-to-clothing interactions. Our findings indicated that skin-to-skin self-touch poses caused significant changes in bioimpedance magnitude at high frequencies (between 237.8 kHz and 4.1 MHz), making them consistently detectable across different individuals. Skin-to-clothing contacts, while discernible, presented more challenges due to the low conductivity and high variability of clothing. Importantly, adversarial mid-air gestures did not cause significant deviations in the bioimpedance magnitude at high frequencies, which is crucial for distinguishing genuine self-touches from nontouch poses.

We attribute our measurement method's higher success at detecting self-touch poses, in particular skin-to-skin contact, and its lower responsiveness to mid-air hand gestures to these poses' *different circuit topologies*. As visible in Figs. 1 and 4, contact between the hands (or with the face or clothing) creates an additional current pathway parallel to the baseline circuit, which decreases the point-to-point bioimpedance magnitude (compare dashed and solid lines at high frequencies in Fig. 5). Conversely, mid-air hand gestures, such as clenching or pinching the fingers, do not create a new current pathway between the wrists, therefore showing bioimpedance magnitude values more similar to the baseline. Between these mid-air gestures, clenching was more detectable due to its increased muscle contraction and skin stretching, two mechanisms that influence bioimpedance measurements [36], [46]. The phase of the bioimpedance detected the highest number of poses with the lowest p-values around 50 kHz (in line with prior work on BIA). However, in this range of frequencies, all clenching poses were also detected, and the clothing material had a significant impact. These results make phase less appealing than magnitude for use in detecting self-touch.

Moreover, we showed that the body parts and the contact area involved in skin-to-skin contacts played a critical role in the bioimpedance magnitude response. The use of one or two hands showed significant differences: in one-handed self-touches, the current has to travel through a longer parallel electrical pathway, which goes from the fingers down through the neck and out the arm, whereas in two-handed self-touches, the shortest parallel pathway goes from one hand to the other either directly or through the face (see Fig. 4). Furthermore, touching the hands directly or through the face differed significantly at some frequencies, despite the similar pathway lengths and contact areas of these two topologies (see Fig. 4). The variability across frequencies is likely due to the softer nature of the cheeks, which led to higher variations in the contact area and applied force compared to the hand-to-hand contacts. Finally, when considering the one-handed self-touches, touching the face with the right or left hand creates a mirrored circuit topology, which could explain their very similar bioimpedance changes. Interestingly, at high frequencies and with large contact areas, the phase showed differences between the usage of the left or right hand, with the right hand showing higher phase values independent of the handedness of the participant.

For the contact size, we observed a systematic decrease in the bioimpedance magnitude with increasing contact size (compare tLR4 and tLR in Fig. 5), as larger contact areas facilitate electrical flow. Furthermore, at high frequencies, the only nonsignificant pairs were in the one-handed facial self-touch poses. Besides the variations due to the softness of the cheeks, the longer path of these poses, compared to the two-handed ones, results in a higher total impedance and, consequently, a smaller deviation from the baseline impedance (see the pink and green lines in Fig. 5), which in turn decreases the relative differences between contact areas. In this phase, the difference between the presence or absence of the face and the use of one or two hands was emphasized even more. Given these results, we believe that subtle differences, such as the use of one or two fingers during one-handed facial contact, may become distinguishable when analyzing the full bioimpedance spectrum rather than examining each frequency independently, closer to the approach used in Touché for classifying poses [18].

Regarding the attributes, our analyses showed that handedness and BMI did not have any significant impact. Instead, sex, ethnicity, clothing, and starting position showed frequency-dependent effects: sex influenced magnitude at low and high frequencies and phase at low frequencies; men are generally larger than women, which will tend to give them higher wrist-to-wrist bioimpedance. Ethnicity and clothing had an impact on the phase at medium frequencies. The phase was also sensitive to the starting position. We believe that the impact of sex at high frequencies, which emerged as the best range to detect only self-touch poses, does not undermine the generalizability of the tested approach. First, our sensitivity analysis indicated that the impact of the sex attribute is minor. Second, this information could easily be provided as an input to the sensing system and is constant for a user, unlike clothing and starting position, whose influence on the phase makes phase even less attractive than magnitude for detecting self-touch.

VI. Limitations and Conclusion

We observed that one of the primary limitations of this sensing method is its lower sensitivity (i.e., lower significance level) in detecting skin-to-clothing contacts compared to skin-to-skin contacts. Unlike skin-to-skin contacts, which create direct conductive pathways, skin-to-clothing interactions introduce complex electrical interfaces, increasing variability in bioimpedance readings. In addition, the diversity of fabrics affects conductivity, leading to inconsistent deviations from the baseline pose. Based on our findings, we believe that other sensing modalities may be more effective for skin-to-clothing detection. However, since our dataset included only three skin-to-clothing poses, a more thorough analysis is necessary before discarding the use of bioimpedance for these contacts. Furthermore, our experiments were conducted under controlled laboratory conditions, allowing us to systematically explore the capabilities of bioimpedance sensing. However, this controlled environment does not reflect the

complexities of dynamic real-world conditions, where external factors, such as drastic temperature fluctuations, may influence both the fabric's conductivity and the changes in the user's bioimpedance. Therefore, future research should focus on testing the studied measurement approach in more naturalistic settings. Additionally, future studies should include participants from a broader range of age groups to better understand the potential influence of age on bioimpedance changes. While our focus was on assessing bioimpedance as a sensing method for self-touch detection, future efforts should prioritize portability and wearability to develop a system that can be used in real-time applications. For example, the sensing unit can be miniaturized [18], and a simpler two-terminal connection could be used (due to the low wire impedance).

We envision this technology playing a crucial role in healthcare, where it could monitor face-touching behaviors in hospitals to mitigate infection risks, especially during outbreaks like COVID-19. In behavioral and psychological research, it could track stress-induced self-touch patterns, providing valuable data for emotional assessments and therapeutic interventions. Such a system could also enhance human–computer interaction by distinguishing between hovering and actual contact in virtual-reality environments.

In conclusion, our findings demonstrate that bioimpedance-based sensing systems can effectively detect skin-to-skin self-touch poses across a diverse range of individuals. This approach performs particularly well when both hands are in contact (whether directly or through another body part) and is especially effective with larger contact areas. Based on our understanding of the underlying physiological mechanisms, we believe this method's ability to detect self-touch is independent of factors like hand shape, contact location, and the specific fingers involved, meaning bioimpedance magnitude at high frequencies can be used to detect skin-to-skin self-touch beyond the chosen set of poses. Our research also opens up exciting possibilities for differentiating between poses involving various body parts and contact sizes. By leveraging these insights, researchers can significantly advance the design and application of bioimpedance technology, paving the way for innovative solutions in health monitoring, human–computer interaction, and beyond. We publicly share the dataset and code associated with this article to allow further investigations of these fascinating phenomena [47].

ACKNOWLEDGMENT

The authors thank Giulia Raimondi for insightful discussions on impedance measurement, Hyosang Lee for input on circuits, Miquel Bosch Bruguera and Philipp Spitzer for recommendations on statistics, and Giulia Ballardini for constructive discussions on various aspects of the project. They also thank the Max Planck Research School for Intelligent Systems (IMPRS-IS) for supporting Maria-Paola Forte.

REFERENCES

[1] S. M. Mueller, S. Martin, and M. Grunwald, "Self-touch: Contact durations and point of touch of spontaneous facial self-touches differ depending on cognitive and emotional load," *PLoS ONE*, vol. 14, no. 3, Mar. 2019, Art. no. e0213677.

[2] A. Kronrod and J. M. Ackerman, "I'm so touched! Self-touch increases attitude extremity via self-focused attention," *Acta Psychol.*, vol. 195, pp. 12–21, Apr. 2019.

[3] J. Rahman, J. Mumin, and B. Fakhruddin, "How frequently do we touch facial T-zone: A systematic review," *Ann. Global Health*, vol. 86, no. 1, p. 75, Jul. 2020.

[4] N. Zhang, W. Jia, P. Wang, M.-F. King, P.-T. Chan, and Y. Li, "Most self-touches are with the nondominant hand," *Sci. Rep.*, vol. 10, no. 1, pp. 1–13, Jun. 2020.

[5] S. M. Kanakri, M. Shepley, J. W. Varni, and L. G. Tassinary, "Noise and autism spectrum disorder in children: An exploratory survey," *Res. Develop. Disabilities*, vol. 63, pp. 85–94, Apr. 2017.

[6] E. van der Kooij, "Contact: A phonological or a phonetic feature of signs?" *Linguistics Netherlands*, vol. 14, pp. 109–122, Aug. 1997.

[7] Y. L. A. Kwok, J. Gralton, and M.-L. McLaws, "Face touching: A frequent habit that has implications for hand hygiene," *Amer. J. Infection Control*, vol. 43, no. 2, pp. 112–114, Feb. 2015.

[8] C. Harrison, D. Tan, and D. Morris, "Skinput: Appropriating the body as an input surface," in *Proc. SIGCHI Conf. Hum. Factors Comput. Syst.*, Atlanta, Georgia. ACM, Apr. 2010, pp. 453–462.

[9] R. Boehme, S. Hauser, G. J. Gerling, M. Heilig, and H. Olausson, "Distinction of self-produced touch and social touch at cortical and spinal cord levels," *Proc. Nat. Acad. Sci. USA*, vol. 116, no. 6, pp. 2290–2299, Feb. 2019.

[10] C. Xu, S. A. Solomon, and W. Gao, "Artificial intelligence-powered electronic skin," *Nature Mach. Intell.*, vol. 5, no. 12, pp. 1344–1355, Dec. 2023.

[11] C. Harrison, H. Benko, and A. D. Wilson, "OmniTouch: Wearable multitouch interaction everywhere," in *Proc. 24th Annu. ACM Symp. User Interface Software Technol.*, 2011, pp. 441–450.

[12] N. Dezfuli, M. Khalilbeigi, J. Huber, F. Müller, and M. Mühlhäuser, "PalmRC: Imaginary palm-based remote control for eyes-free television interaction," in *Proc. 10th Eur. Conf. Interact. TV Video*, Berlin, Germany, Jul. 2012, pp. 27–34.

[13] G. Laput, R. Xiao, X. Chen, S. E. Hudson, and C. Harrison, "Skin buttons: Cheap, small, low-powered and clickable fixed-icon laser projectors," in *Proc. 27th Annu. ACM Symp. User Interface Softw. Technol.*, Honolulu, Hawaii, Oct. 2014, pp. 389–394.

[14] M. Fieraru, M. Zanfir, E. Oneata, A.-I. Popa, V. Olaru, and C. Sminchisescu, "Learning complex 3D human self-contact," in *Proc. AAAI Conf. Artif. Intell. (AAAI)*, vol. 35, May 2021, pp. 1343–1351.

[15] L. Müller, A. A. A. Osman, S. Tang, C.-H. P. Huang, and M. J. Black, "On self-contact and human pose," in *Proc. IEEE Conf. Comput. Vis. Pattern Recognit.*, Jun. 2021, pp. 9990–9999.

[16] A. Mujibiya, X. Cao, D. S. Tan, D. Morris, S. N. Patel, and J. Rekimoto, "The sound of touch: On-body touch and gesture sensing based on transdermal ultrasound propagation," in *Proc. ACM Int. Conf. Interact. Tabletops Surf.* St. Andrews, U.K.: ACM, Oct. 2013, pp. 189–198.

[17] Y. Zhang, J. Zhou, G. Laput, and C. Harrison, "SkinTrack: Using the body as an electrical waveguide for continuous finger tracking on the skin," in *Proc. CHI Conf. Hum. Factors Comput. Syst.*, San Jose, CA, USA, May 2016, pp. 1491–1503.

[18] M. Sato, I. Poupyrev, and C. Harrison, "Touché: Enhancing touch interaction on humans, screens, liquids, and everyday objects," in *Proc. SIGCHI Conf. Hum. Factors Comput. Syst.*, Austin, TX, USA, May 2012, pp. 483–492.

[19] R. Hajika et al., "RadarHand: A wrist-worn radar for on-skin touch-based proprioceptive gestures," *ACM Trans. Comput.-Hum. Interact.*, vol. 31, no. 2, pp. 1–36, Apr. 2024.

[20] U. G. Kyle et al., "Bioelectrical impedance analysis—Part I: Review of principles and methods," *Clin. Nutrition*, vol. 23, no. 5, pp. 1226–1243, Oct. 2004.

[21] R. Baghbani, M. B. Shadmehr, M. Ashoorirad, S. F. Molaeezadeh, and M. H. Moradi, "Bioimpedance spectroscopy measurement and classification of lung tissue to identify pulmonary nodules," *IEEE Trans. Instrum. Meas.*, vol. 70, pp. 1–7, 2021.

[22] S. F. Scagliusi et al., "Bioimpedance spectroscopy-based edema supervision wearable system for noninvasive monitoring of heart failure," *IEEE Trans. Instrum. Meas.*, vol. 72, pp. 1–8, 2023.

[23] J. Chen, L. Ke, Q. Du, Y. Zheng, and Y. Liu, "Cerebral blood flow autoregulation measurement via bioimpedance technology," *IEEE Trans. Instrum. Meas.*, vol. 71, pp. 1–8, 2022.

[24] T.-W. Wang, W.-X. Chen, H.-W. Chu, and S.-F. Lin, "Single-channel bioimpedance measurement for wearable continuous blood pressure monitoring," *IEEE Trans. Instrum. Meas.*, vol. 70, pp. 1–9, 2021.

[25] P. Arpaia, F. Mancino, and N. Moccaldi, "A reproducible bioimpedance transducer for insulin noninvasive measurement," *IEEE Trans. Instrum. Meas.*, vol. 72, pp. 1–11, 2023.

[26] Y. Vardar and K. J. Kuchenbecker, "Finger motion and contact by a second finger influence the tactile perception of electrovibration," *J. Roy. Soc. Interface*, vol. 18, no. 176, Mar. 2021, Art. no. 20200783.

[27] B. Jensen et al., "Ethnic differences in fat and muscle mass and their implication for interpretation of bioelectrical impedance vector analysis," *Appl. Physiol., Nutrition, Metabolism*, vol. 44, no. 6, pp. 619–626, Jun. 2019.

[28] M. Dittmar, "Reliability and variability of bioimpedance measures in normal adults: Effects of age, gender, and body mass," *Amer. J. Phys. Anthropol.*, vol. 122, no. 4, pp. 361–370, Dec. 2003.

[29] S. F. Khalil, M. S. Mohktar, and F. Ibrahim, "The theory and fundamentals of bioimpedance analysis in clinical status monitoring and diagnosis of diseases," *Sensors*, vol. 14, no. 6, pp. 10895–10928, 2014.

[30] D. Naranjo-Hernández, J. Reina-Tosina, and M. Min, "Fundamentals, recent advances, and future challenges in bioimpedance devices for healthcare applications," *J. Sensors*, vol. 2019, pp. 1–42, Jul. 2019.

[31] L. C. Ward, "Bioelectrical impedance analysis for body composition assessment: Reflections on accuracy, clinical utility, and standardisation," *Eur. J. Clin. Nutrition*, vol. 73, no. 2, pp. 194–199, Feb. 2019.

[32] P. Deurenberg, J. A. Weststrate, I. Paymans, and K. Van der Kooy, "Factors affecting bioelectrical impedance measurements in humans," *Eur. J. Clin. Nutrition*, vol. 42, no. 12, pp. 1017–1022, Dec. 1988.

[33] W. D. Evans, H. McClagish, and C. Trudgett, "Factors affecting the in vivo precision of bioelectrical impedance analysis," *Appl. Radiat. Isot.*, vol. 49, nos. 5–6, pp. 485–487, May 1998.

[34] E. Gualdi-Russo and S. Toselli, "Influence of various factors on the measurement of multifrequency bioimpedance," *HOMO*, vol. 53, no. 1, pp. 1–16, 2002.

[35] J. R. Matthie, "Bioimpedance measurements of human body composition: Critical analysis and outlook," *Expert Rev. Med. Devices*, vol. 5, no. 2, pp. 239–261, Mar. 2008.

[36] E. M. Bartels, E. R. Sørensen, and A. P. Harrison, "Multi-frequency bioimpedance in human muscle assessment," *Physiological Rep.*, vol. 3, no. 4, Apr. 2015, Art. no. e12354.

[37] F. Campa, S. Toselli, M. Mazzilli, L. A. Gobbo, and G. Coratella, "Assessment of body composition in athletes: A narrative review of available methods with special reference to quantitative and qualitative bioimpedance analysis," *Nutrients*, vol. 13, no. 5, p. 1620, May 2021.

[38] R. J. Mathews and E. Jovanov, "Enabling complex impedance spectroscopy for cardio-respiratory monitoring with wearable biosensors: A case study," *Electrochem*, vol. 4, no. 3, pp. 389–410, Aug. 2023.

[39] Zurich Instrum. AG. (2022). *ziMFIA User Manual*. Accessed: Sep. 30, 2024. [Online]. Available: https://docs.zhinst.com/pdf/ziMFIA_UserManual.pdf

[40] R. Buendia, R. Gil-Pita, and Y. F. Seoane, "Cole parameter estimation from total right side electrical bioimpedance spectroscopy measurements—Influence of the number of frequencies and the upper limit," in *Proc. Annu. Int. Conf. IEEE Eng. Med. Biol. Soc. (EMBS)*, Aug. 2011, pp. 1843–1846.

[41] M. Hosseini, T. Ihmels, Z. Chen, M. Koelle, H. Müller, and S. Boll, "Towards a consensus gesture set: A survey of mid-air gestures in HCI for maximized agreement across domains," in *Proc. CHI Conf. Hum. Factors Comput. Syst.*, Apr. 2023, pp. 1–24.

[42] World Health Org. (2010). *A Healthy Lifestyle-WHO Recommendations*. [Online]. Available: https://www.who.int/europe/news-room/fact-sheets/item/a-healthy-lifestyle---who-recommendations

[43] J. W. S. Hearle, "The electrical resistance of textile materials: A review of the literature," *J. Textile Inst. Proc.*, vol. 43, no. 4, pp. P194–P223, Apr. 1952.

[44] H. Schielzeth et al., "Robustness of linear mixed-effects models to violations of distributional assumptions," *Methods Ecol. Evol.*, vol. 11, no. 9, pp. 1141–1152, Jun. 2020.

[45] M. E. Glickman, S. R. Rao, and M. R. Schultz, "False discovery rate control is a recommended alternative to Bonferroni-type adjustments in health studies," *J. Clin. Epidemiol.*, vol. 67, no. 8, pp. 850–857, Aug. 2014.

[46] H. D. Talhouet and J. G. Webster, "The origin of skin-stretch-caused motion artifacts under electrodes," *Physiol. Meas.*, vol. 17, no. 2, pp. 81–93, May 1996.

[47] M.-P. Forte, Y. Vardar, B. Javot, and K. J. Kuchenbecker, "Dataset and code for 'wrist-to-wrist bioimpedance can reliably detect discrete self-touch,'" Edmond, V1, 2025. [Online]. Available: https://doi.org/10.17617/3.P0NEOF

Maria-Paola Forte (Graduate Student Member, IEEE) received the B.Sc. degree in biomedical engineering from the University of Genova, Genoa, Italy, in 2015, and the M.Sc. degree in biomedical engineering from Politecnico di Milano, Milan, Italy, in 2018, with a focus on electronic technologies. She is currently pursuing the Ph.D. degree in computer science with the Max Planck Institute for Intelligent Systems, Stuttgart, Germany.

Since 2017, she has been with the Max Planck Institute for Intelligent Systems, where she initially worked as a Research Engineer. Her research focuses on developing technologies to assist individuals with sensory or motor impairments and to enhance human performance in highly specialized tasks, such as robotic surgery. Her work integrates vision-based and sensor-based methods across the reality–virtuality continuum.

Yasemin Vardar (Member, IEEE) received the B.Sc. degree in mechatronics engineering from Sabancı University, Istanbul, Turkey, in 2010, the M.Sc. degree in systems and control from Eindhoven University of Technology, Eindhoven, The Netherlands, in 2012, and the Ph.D. degree in mechanical engineering from Koç University, Istanbul, in 2018.

She is an Assistant Professor at Delft University of Technology, Delft, The Netherlands. Before joining Delft, she was a Post-Doctoral Researcher at the Max Planck Institute for Intelligent Systems, Stuttgart, Germany. Her research interests focus on understanding how tactile information translates into human perception and how these sensory experiences can be effectively simulated in digital environments.

Dr. Vardar has been recognized with several prestigious awards, including the NWO VENI Award in 2021 and the Eurohaptics Best Ph.D. Thesis Award in 2018. She serves as the Chair for the Technical Committee on Haptics.

Bernard Javot (Member, IEEE) received the master's degree in robotics and the Ph.D. degree in haptics from Université Pierre et Marie Curie, Paris, France, in 2011 and 2016, respectively.

He joined the Max Planck Institute for Intelligent Systems, Stuttgart, Germany, where he works as a Senior Research Engineer. He earned the Highest-Level Teaching Accreditation, in France, in 2005 and worked as a Manufacturing Teacher, in Paris, for ten years. His research interests include inventing actuators and sensors for haptics.

Katherine J. Kuchenbecker (Fellow, IEEE) received the B.S., M.S., and Ph.D. degrees in mechanical engineering from Stanford University, Stanford, CA, USA, in 2000, 2002, and 2006, respectively.

She was a Post-Doctoral Researcher in the Johns Hopkins University, Baltimore, MD, USA, and an Assistant Professor and an Associate Professor in the GRASP Laboratory, University of Pennsylvania, Philadelphia, PA, USA, from 2007 to 2016. Since 2017, she has been a Director at the Max Planck Institute for Intelligent Systems, Stuttgart, Germany. Her research blends robotics and human–computer interaction, including work in haptics, teleoperation, physical human–robot interaction, tactile sensing, and medical applications.

Dr. Kuchenbecker has been honored with the 2009 NSF CAREER Award, the 2012 IEEE RAS Academic Early Career Award, and a 2014 Penn Lindback Award for Distinguished Teaching.